

Full length article

Element interactions of cold-formed stainless steel cross-sections subjected to combined compression and bending

Feng Zhou^{a,b,*}, Zhi Chen^b^a State Key Laboratory of Disaster Reduction in Civil Engineering, Tongji University, Shanghai 200092, China^b Department of Structural Engineering, Tongji University, 1239 Siping Road, Shanghai 200092, China

ARTICLE INFO

Keywords:

Beam-columns
Cold-formed stainless steel
Local buckling
Interaction effects of constituent plate elements
Tubular section

ABSTRACT

A comprehensive numerical investigation of cold-formed stainless steel cross-sections subjected to combined compression and bending is presented in this paper. A non-linear finite element model (FEM) including geometric and material non-linearities was developed using the finite element package ABAQUS. Upon validation of the FEM, the model was then used for an extensive parametric study to investigate the interaction effects of constituent plate elements of cold-formed stainless steel square and rectangular hollow section beam-columns.

The investigation indicates that the interaction effects of constituent plate elements on cross-section response are obvious particularly for slender sections. Current design provisions on Class 3 and Class 2 slenderness limits and effective width equations specified in American Specification, EC3 code and proposed by Gardner are not suitable for square and rectangular stainless steel hollow section beam-columns since the interaction effects of constituent plate elements are ignored. The new Class 3 and Class 2 slenderness limits and the section capacity design equations based on the whole cross-section response enable more accurate prediction of local buckling, thus allowing better utilization of material and more economic design.

1. Introduction

Stainless steel is being increasingly used in structural applications due to its favourable durability, ductility, weldability, aesthetic appearance, as well as improved fire resistance [1]. In addition, stainless steel is very suitable for cold processing due to its pronounced strain hardening. A cold-formed hollow section is formed by rolling an annealed flat strip into a circular hollow section, which is then welded at the edges. The process is completed by further rolling into a square or rectangular hollow section (SHS or RHS).

Over the past decades, extensive investigations have been conducted on cold-formed stainless steel tubular members subjected to combined compression and bending. At section level, Zhao et al. [2–4] conducted experimental and numerical studies on cold-formed stainless steel SHS and RHS stub beam-columns, and it was revealed that the current design standards can significantly under-estimate the resistance of stainless steel cross-sections in combined compression and bending. Mohammad et al. [5] examined the behavior of slender stainless steel cross-sections subjected to combined compression and bending, based on which the Continuous Strength Method (CSM) was developed. Apart from the tests and analysis on stub beam-columns, slender stainless steel beam-columns were investigated by Huang and Young [6], Liu

et al. [7] and Zhao et al. [8]. It was commonly found that the code predictions are mostly conservative for stainless steel beam-columns with rooms for improvement in the current design guidance.

For cold-formed stainless steel members having relatively large width-to-thickness ratios, the plate elements may buckle locally when loaded in compression. The proneness to buckle of any plate element within the cross-section may limit the section capacity by preventing the attainment of the yield strength. The previous studies [9–14] show that the cross-section response is not only assumed to the behavior of its most slender plate element in the cross-section but also depends on the aspect ratio and stress state of the cross-section. The interaction effects of constituent plate elements on cross-section response are very obvious regarding the slenderness limits and the cross-section ultimate resistances for cold-formed stainless steel SHSs and RHSs. Zhou et al. [15] and Zhou and Long [16] investigated the plate element interactions of cold-formed stainless steel SHSs and RHSs subjected to pure axial compression and pure bending, respectively. It was shown that the interaction effects of constituent plate elements on cross-section response were quite obvious particularly for slender sections. The new Class 3 and Class 2 slenderness limits and the cross-section capacity design equations were proposed based on the whole cross-section response, carefully considering the interaction effects of constituent plate

* Corresponding author at: State Key Laboratory of Disaster Reduction in Civil Engineering, Tongji University, Shanghai 200092, China.

E-mail address: zhoufeng@tongji.edu.cn (F. Zhou).

elements.

A number of early research outcomes have promoted the development of major stainless steel design codes, including the ASCE Specification [17] for the Design of Cold-formed Stainless Steel Structural Members and the EC3 Code [18] Design of Steel Structures, Part 1.4: Supplementary Rules for Stainless Steels. The cross-section classification approach, aiming at identifying the extent to which the resistance and possibly the rotation capacity of cross-sections are limited by possible local buckling of the compression plate elements composing that section, is employed in the EC3 Code as a means of codified treatment for local buckling of cross-sections that are partly or fully in compression. However, the EC3 code treats the plate elements in the cross-section individually, neglecting the constituent plate elements interaction.

The purpose of this paper is to thoroughly investigate the plate element interaction of cold-formed stainless steel SHSs and RHSs subjected to combined compression and bending. Firstly, an accurate and efficient non-linear finite element model was developed to simulate the cross-section response of cold-formed stainless steel SHSs and RHSs subjected to combined compression and bending. The initial local imperfection and non-linear material properties of the flat and corner portions of the cross-section have been carefully incorporated into the finite element model (FEM). Secondly, upon validation of the FEM, an extensive parametric study on a range of cross-section aspect ratio and stress ratio was performed. Thirdly, the plate element interaction of cold-formed stainless steel SHSs and RHSs under combined compression and bending was investigated. The design provisions on Class 3 and Class 2 slenderness limits and effective width formulae specified in the current ASCE Specification [17], EC3 Code [18] and proposed by Gardner and Theofanous [19] were assessed based on the results of the parametric study. Lastly, new Class 3 and Class 2 slenderness limits and the section capacity design equations based on the whole cross-section response, carefully taking into account the interaction effects of constituent plate elements, were proposed in this study for cold-formed stainless steel SHSs and RHSs subjected to combined compression and bending.

2. Summary of experimental investigation

The experimental investigation performed by Zhao et al. [2] reported the tests of cold-formed stainless steel square and rectangular hollow sections (SHS & RHS) under combined compression and bending, which were used to verify the finite element model developed in this paper. Five cross-section sizes were tested, which were S100 × 100 × 5, S120 × 120 × 5, S150 × 150 × 8, R100 × 150 × 6 and R150 × 100 × 8. The length of the test specimen (L) was chosen to avoid member buckling. The measured test specimen dimensions are summarized in Table 1 using the nomenclature defined in Fig. 1.

The specimens are labeled according to their nominal dimensions and stress state. For example, the label “S150 × 100 × 8-ψ0.22” defines the specimen having square hollow section with nominal overall depth of the web (H) of 150 mm, overall flange width (B) of 100 mm and thickness (t) of 8 mm. The cross-section stress ratio ψ under elastic stage equals to 0.22 and ψ is defined by Eq. (1).

$$\psi = \frac{\sigma_{\min}}{\sigma_{\max}} \quad (1)$$

where σ_{\min} and σ_{\max} are the cross-section minimum and maximum stresses under elastic stage, respectively, as shown in Fig. 2. The cross-section stress is positive if in compression, otherwise, the reverse. If the specimen is subjected to pure axial compression, the cross-section stress ratio ψ equals to 1.0. If the specimen is subjected to pure bending, the cross-section stress ratio ψ equals to -1.0. For the specimens under combined compression and bending considered in this study, the cross-section stress ratio ranges from 1.0 to -1.0.

The material properties of the flat and corner portions of the

Table 1
Summary of test specimens [2].

| Specimen | L (mm) | B (mm) | H (mm) | t (mm) | r_i (mm) | e_o (mm) |
|-----------------------|-------------|-------------|-------------|-------------|---------------|---------------|
| S100 × 100 × 5-ψ 0.25 | 350.0 | 99.9 | 100.0 | 4.65 | 2.1 | 17.9 |
| S100 × 100 × 5- ψ0.07 | 350.0 | 100.0 | 100.0 | 4.70 | 2.2 | 25.8 |
| S100 × 100 × 5-ψ-0.28 | 350.0 | 100.0 | 100.0 | 4.66 | 2.1 | 52.9 |
| S120 × 120 × 5- ψ0.57 | 399.9 | 120.1 | 120.2 | 4.65 | 5.8 | 10.0 |
| S120 × 120 × 5-ψ-0.02 | 400.0 | 120.1 | 120.0 | 4.61 | 5.7 | 38.0 |
| S120 × 120 × 5-ψ-0.30 | 400.0 | 120.0 | 120.0 | 4.61 | 5.8 | 68.0 |
| R100 × 150 × 6-ψ-0.05 | 350.1 | 100.1 | 150.1 | 5.85 | 7.0 | 44.8 |
| R100 × 150 × 6-ψ-0.23 | 449.8 | 100.0 | 150.4 | 5.85 | 7.1 | 64.1 |
| R100 × 150 × 6-ψ-0.39 | 450.1 | 99.9 | 150.1 | 5.82 | 7.0 | 92.4 |
| R100 × 150 × 6-ψ-0.52 | 450.0 | 100.0 | 150.2 | 5.90 | 7.1 | 128.4 |
| R150 × 100 × 8-ψ0.22 | 450.0 | 150.1 | 100.0 | 7.73 | 9.6 | 19.9 |
| R150 × 100 × 8-ψ-0.25 | 450.2 | 150.1 | 100.1 | 7.70 | 9.6 | 51.6 |
| R150 × 100 × 8-ψ-0.42 | 450.0 | 150.1 | 100.0 | 7.71 | 9.7 | 74.9 |
| S150 × 150 × 8- ψ0.20 | 449.8 | 150.0 | 150.2 | 8.00 | 11.1 | 29.5 |
| S150 × 150 × 8-ψ-0.08 | 450.0 | 150.0 | 150.1 | 7.99 | 11.2 | 51.6 |
| S150 × 150 × 8-ψ-0.32 | 450.0 | 150.0 | 150.0 | 8.02 | 11.2 | 84.2 |

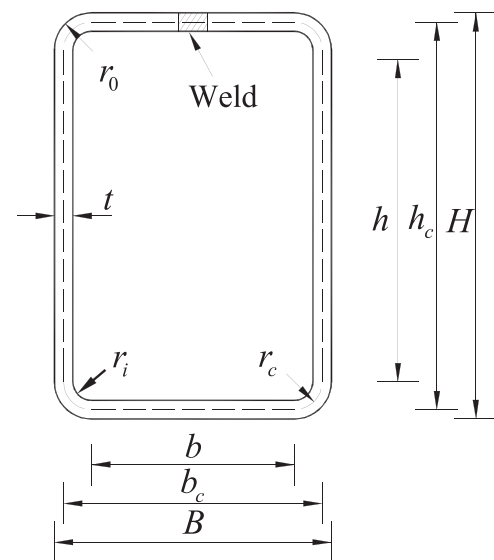


Fig. 1. Definition of symbols.

specimens were determined by tensile coupon tests. For each cross-section size, two flat coupons taken from the center of the face at 90° angle from the weld and two corner coupons taken from the curved corner regions opposite to the weld in the longitudinal direction of the untested specimens were tested. All the tensile coupon tests were conducted using Zwick/Roell Z100 kN electromechanical testing machine according to the requirements of EN ISO 6892-1 [20]. The measured averaged material properties of the flat and corner portions are summarized in Table 2, including the initial Young's Modulus E , the 0.2% tensile stress $\sigma_{0.2}$, the 1.0% tensile stress $\sigma_{1.0}$, the ultimate tensile strength σ_u , the strain at the ultimate tensile strength ϵ_u , the plastic strain at fracture over the standard gauge length ϵ_f and strain hardening exponents n and $n'_{0.2,1.0}$, which are used in the improved compound Ramberg-Osgood (R-O) material model [21,22].

An AMSER 5000 kN hydraulic testing machine with hemispherical bearings at both ends providing pin-ended conditions in any conditions was used to apply an eccentric compression load to the specimen. The value of ψ could be obtained by varying the initial load eccentricity (e_o). Displacement control was adopted at a constant speed of 0.1 mm/min for all beam-column specimens. The key experimental results including the ultimate loads (N_{u-Test}) and the corresponding end rotation at failure (ϕ_{u-Test}) are listed in Table 3. The stub beam-column tests are detailed in Zhao et al. [2].

Download English Version:

<https://daneshyari.com/en/article/6777265>

Download Persian Version:

<https://daneshyari.com/article/6777265>

[Daneshyari.com](https://daneshyari.com)